# Reversible Swelling Process of Sixth-Generation Poly(amido amine) Dendrimers Molecule As Determined by Quartz Crystal Microbalance Technique

**ARTICLE** *in* THE JOURNAL OF PHYSICAL CHEMISTRY C · JANUARY 2013

Impact Factor: 4.77 · DOI: 10.1021/jp307832p



**3 AUTHORS**, INCLUDING:

Barbara Jachimska
Polish Academy of Sciences
**38** PUBLICATIONS **623** CITATIONS
SEE PROFILE

Szczepan Zapotoczny
Jagiellonian University
**91** PUBLICATIONS **1,179** CITATIONS
SEE PROFILE

THE JOURNAL OF PHYSICAL CHEMISTRY C

Article

pubs.acs.org/JPCC

# Reversible Swelling Process of Sixth-Generation Poly(amido amine) Dendrimers Molecule As Determined by Quartz Crystal Microbalance Technique

Barbara Jachimska,*[,†] Marta Łapczyńska,[†] and Szczepan Zapotoczny[‡]

[†]J. Haber Institute of Catalysis and Surface Chemistry, PAS, Niezapominajek 8, 30-239 Cracow, Poland

[‡]Faculty of Chemistry, Jagiellonian University, Ingardena 3, 30-060 Cracow, Poland

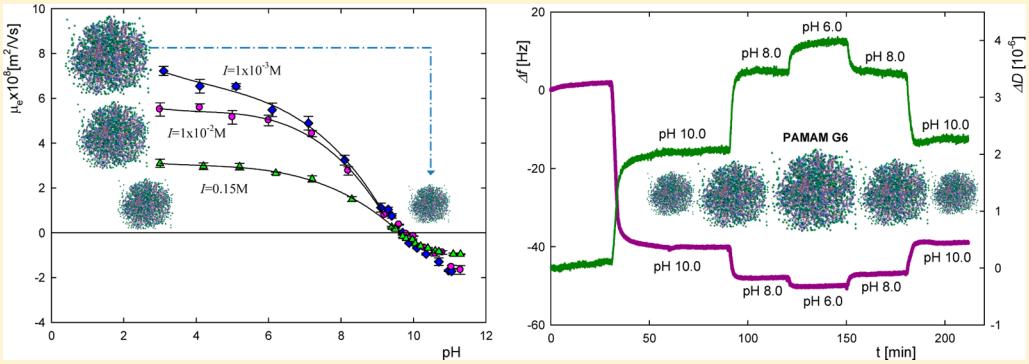


**ABSTRACT:** Dynamic light scattering (DLS) was used to measure the electrophoretic mobility and diffusion coefficients of sixth-generation poly(amido amine), G6 PAMAM, dendrimers in an aqueous solution. The measurements were used to determine the effective charge and the hydrodynamic radius of PAMAM molecules. The physicochemical measurements were supplemented with dynamic viscosity measurements. From these data, the intrinsic viscosity of the PAMAM solutions was determined. The viscosity behavior was discussed in terms of the core/shell dendrimer structure postulated in the literature. Additional information about the structure of the dendrimers was obtained using atomic force microscopy (AFM) and a quartz crystal microbalance (QCM). The latter was used to study the adsorption of G6 PAMAM from aqueous solution on a Au-coated surface. The QCM measurements indicate that the adsorbed dendrimer molecules significantly change their conformation and viscoelastic properties in response to variations in ionic strength and solution pH. We demonstrated that the QCM method detects the reversible swelling of dendrimer molecules in the film due to its adoption of an extended conformation upon the protonation of the dendrimer's amine groups.

## INTRODUCTION

Dendrimers are a specific class of polymers with highly branched and regular structures that are produced by either divergent or convergent synthesis methodologies.[1] Different synthetic methodologies lead to the formation of monodispersed nanoparticles with controlled dimensions that increase with the generation number and specific surface functionalization. The study of dendrimer properties is still in its infancy as compared to that of classical polymers, and there is still a large information gap that must be bridged before the potential applications of these new materials can be realized. It also involves surfaces modified with dendrimers. In practice, such surfaces may provide a valuable alternative to those modified by self-assembled monolayers of linear polymers.

The surface functional groups located in the outermost dendrimer layer significantly influence the physical and chemical properties of dendrimers. Their versatile structures allow for embedding nonpolar or charged guest molecules in dendrimer internal voids or on its surface due to electrostatic interactions.[2] The structural properties of dendrimers have been investigated using both theoretical[3−5] and experimental methods.[1,6−8] The experimental studies of dendrimers have been carried out using different techniques such as small-angle neutron scattering (SANS),[6] small-angle X-ray scattering (SAXS),[7] atomic force spectroscopy (AFM),[8] and transmission electron microscopy (TEM).[1]

One of the most studied dendrimers is poly(amido amine), PAMAM, containing primary amine groups in the outermost layer. Detailed scattering experiments (SANS) have revealed the swelling of PAMAM dendrimers in aqueous solution, both upon pH and a substantial change of salt concentration, is very limited. SANS investigations on eighth-generation (G8) PAMAM dendrimer showed only ca. 2% increase of its radius of gyration ($R_g$) upon the pH change from 10.1 to 4.7.[6] These measurements suggest that the electrostatically driven swelling of dendrimers of sufficiently high generation is inhibited due to

**Received:** August 7, 2012
**Revised:** December 7, 2012
**Published:** December 27, 2012

steric crowding of the terminal groups. In contrast, molecular dynamics (MD) and Monte Carlo simulations show a significant increase of $R_g$ of PAMAM dendrimers upon increase of pH.[3−5] Maiti et al.,[3] who studied theoretically the structure of G8 PAMAM dendrimers by applying molecular dynamics (MD) simulations, observed a 13% increase in the radius of gyration with the pH change from 12 to 4. However, for the lower generation (G4−G6) PAMAM dendrimers, they found even larger effects (33%).[3] Welch and Methukumar[5] demonstrated, using Monte Carlo simulations, that the shape of the intermolecular density profile of dendrimers in solution can be tailored by varying the ionic strength or pH of the solvent.

Liu et al.[9] combined SANS and SAXS measurements to investigate the structural characteristics of aqueous solution of G7 and G8 PAMAM dendrimers as a function of their protonation. They observed an increase in the molecular size and a continuous variation of the intramolecular density profile upon increasing the protonation. These studies partially resolve the discrepancy between theory and experimental results for the high-generation polyelectrolyte dendrimers.

Over the past decade, much research has been focused on the application of dendrimers in biomedical fields, including drug delivery and gene delivery, cancer-targeting therapy, and diagnosis.[10] Dendrimer-based drug delivery systems are particularly promising because these nanocarriers solubilize some drug molecules, which may be slowly released from the matrix. This may effectively improve the bioavailability of drugs and ensure their precise delivery to targeted tissues or organs. Recently, much attention has been also devoted to the use of dendrimers as building blocks for construction of thin films using the layer-by-layer technique.[11−13]

To apply dendrimers as drug delivery carriers, one must gain reliable information on their properties in the bulk solution and also on adsorption of these molecules on model surfaces. Although there is extensive literature dedicated to linear polymers, only a limited number of investigations have been performed so far on the adsorption of hyperbranched polymers such as dendrimers on solid supports.[14] In view of present knowledge, it is of particular importance to study the adsorption of dendrimers from solutions of various ionic strength and pH.

The phenomenon of swelling dendrimer films adsorbed on a $SiO_2$ surface from salt-free, aqueous solution, was preliminarily investigated and reported for G10 PAMAM dendrimer, using the QCM and AFM techniques.[15] Despite numerous investigations on this phenomenon, swelling of a dendrimer adsorbed onto a solid support is far from being understood in detail. As suggested in ref 15, the phenomenon is strongly influenced by the adsorbate−substrate interactions; hence, the kind of support used and its susceptibility to changing the surface charge with pH may be of great influence on the observed results.

In this work, we used dynamic laser scattering (DLS) and viscosity measurements to characterize in detail the properties of G6 PAMAM dendrimers in electrolyte solutions. These measurements were supplemented by electrophoretic mobility measurements, which allowed us to determine the isoelectric point and the uncompensated (electrokinetic) charge of the dendrimers. These results provide insight into the dynamic structure of PAMAM dendrimers in solutions. Further, we used the quartz crystal microbalance (QCM) for quantitative studies on the formation of G6 PAMAM monolayers on gold. We found that the thickness of the PAMAM films depends strongly on the pH and ionic strength of the solution that influences swelling of the PAMAM films. Our results supply the first compelling experimental evidence for significant swelling of G6 PAMAM dendrimer upon its protonation at the solid/solution interface. This phenomenon is a consequence of spatial relocation of the dendrimer amide groups due to the interactions of the positively charged amines with the oppositely charged condensed counterions and the penetrating water molecules. Insight into the interfacial phenomena is essential for designing materials dedicated to biological applications.

## EXPERIMENTAL SECTION

**Materials.** Sixth-generation (G6) poly(amido amine) (PAMAM) ($M$ = 58 kDa, diagnostic grade) dendrimers in aqueous solutions (9.4% concentration) were obtained from Dendritech (Midland). Solutions were prepared by diluting the starting solution with deionized water, adjusting the pH by adding HCl or NaOH, and adjusting the ionic strength using NaCl.

Mica sheets provided by Mica & Micanite Supplies Ltd. England were used as the reference adsorbing surfaces. The sheets were freshly cleaved before each experiment and used without any pretreatment.

**Methods.** *Dynamic Light Scattering and Electrophoretic Mobility Measurements.* The dendrimer size was determined by dynamic light scattering (DLS) using a Zetasizer Nano ZS Malvern instrument with a measurement range spanning from 0.6 nm to 6 $\mu$m. The Nano ZS instrument incorporates noninvasive backscatter (NIBS) optics. This technique measures the time-dependent fluctuations in the intensity of scattered light that occur as particles undergo Brownian motion.

The electrophoretic mobility was measured using a Zetasizer Nano ZS instrument to conduct laser Doppler velocimetry (LDV); the instrument has a measurement range spanning from 3 nm to 10 $\mu$m. In this technique, a voltage is applied across a pair of electrodes that are placed at both ends of a cell that contains particle dispersion. Charged particles are attracted to the oppositely charged electrode, and their velocity is measured and expressed per unit field strength as the electrophoretic mobility, $\mu_e$.

*Viscosity Measurements.* The dynamic viscosity of the dendrimer solutions was measured using a capillary viscometer equipped with a conductivity sensor to detect the solution level according to the procedure described previously in ref 16. The device was calibrated using pure liquids of known viscosity. The precision of the viscosity measurements, which were able to detect viscosities in the range of 1−10 mPa·s, was estimated to be 0.5%. Concentration of the dendrimer solutions used in the viscosity measurements varied between 40 and 10 000 ppm. The density of the dendrimer solutions was measured using a pycnometer.

*Atomic Force Microscopy (AFM).* For the AFM analysis, G6 PAMAM dendrimers were adsorbed onto mica by immersing the mica substrate into a dendrimer solution of suitable ionic strength and pH. These samples were then rinsed in double-distilled water and dried under a gentle nitrogen stream. Atomic force microscopy (AFM) (Picoforce, Bruker, U.S.) in tapping mode was used to characterize the samples in air. Standard silicon cantilevers (Bruker) with a nominal spring


dx.doi.org/10.1021/jp307832p | J. Phys. Chem. C 2013, 117, 1136−1145

constant of 40 N/m and a tip radius of <10 nm were used for all of the measurements.

*Quartz Crystal Microbalance with Dissipation (QCM-D).* Quartz crystal microbalances with dissipation (QCM-D) have been used extensively over the past decade to investigate protein adsorption[17] and to study the formation of polyelectrolyte multilayers.[18] The QCM sensor is a thin piece of disc-shaped piezoelectric quartz crystal with metal electrodes deposited on both sides. When an RF voltage is applied across the electrodes near the resonant frequency, the crystal oscillates in the thickness-shear mode at its fundamental resonant frequency. The resonant frequency of the crystal is recorded in real time and depends on the total oscillating mass and properties of the quartz crystal. A small mass added to the electrodes induces a decrease in the resonant frequency ($\Delta f = f - f_o$), which is proportional to the mass ($\Delta m$). For flat, uniform, and rigid films, the change in the resonance frequency $\Delta f$ is directly proportional to the adsorbed mass ($\Delta m$) in what is normally referred to as the Sauerbrey equation:

$$\Delta m = -C\frac{\Delta f}{n} \tag{1}$$

where $C$ is the constant of the crystal, which is equal to 17.7 ng/cm$^2$·Hz based on the physical properties of quartz crystal, and $n$ is the overtone number. In the QCM experiment, the changes in the frequency and the energy dissipation upon the adsorption of films are simultaneously measured. According to the Sauerbrey equation, a decrease in the frequency of the crystal oscillations indicates that a mass is adsorbed onto the crystal surface.

In a QCM-D experiment, the decay of the crystal oscillations is also monitored to obtain the energy dissipation, $D_{dis}$, which is related to the viscoelastic properties of the material according to the following equation:

$$D_{dis} = \frac{E_{dis}}{2\pi E_{stor}} \tag{2}$$

where $E_{dis}$ is the energy lost during one oscillation, and $E_{stor}$ is the energy stored in the oscillating circuit. For an adsorbed layer with high rigidity, no change in the dissipation will be observed as a function of adsorption time. However, for an adsorbed viscoelastic layer, the energy dissipating through the layer will increase. Therefore, the change in dissipation provides a semiquantitative measure of the relative stiffness or conformation of an adsorbed layer.

We used gold-coated QCM-D sensors. The dendrimer layer was grown on the QCM crystal by flowing a dendrimer solution with a concentration of $c$ = 5 ppm, an ionic strength of $I = 1 \times 10^{-2}$ M (or $I$ = 0.15 M NaCl), and a pH of 10.0 for 30 min. The QCM sensor was then rinsed with a NaCl solution pH = 10.0 ($I = 1 \times 10^{-2}$ M or 0.15 M NaCl) for 30 min. The pH of the NaCl solution was decreased to 8.0 and finally to 6.0.

## RESULTS AND DISCUSSION

**Diffusion Coefficient.** The diffusion coefficients of the G6 PAMAM dendrimers were measured as a function of the concentration (from 500 to 4000 ppm), pH, and ionic strength. The influence of the pH on the diffusion coefficient was determined at $I$ = 0.15 M in the pH range of 3.5−9.3. Additionally, it was measured for ionic strengths ranging from 0.001 to 0.15 M at a constant pH of 9.5. The diffusion coefficient was found to be $5.7 \times 10^{-7}$ cm$^2$ s$^{-1}$ for ionic strengths larger than 0.01 M and was largely independent of concentration. A higher value of the diffusion coefficient, $7.6 \times 10^{-7}$ cm$^2$ s$^{-1}$, was found only at low ionic strengths.

Molecular simulations (MD)[3,4] show a dependence of the size of the dendrimers on the degree of their protonation. Unfortunately, this difference cannot be detected by the DLS method because its detection limit is close to the dendrimers size. The simulations show structural flexibility and the ability to redistribute mass from the central to outer regions of the dendrimer as well as interdendrimer interactions, which are non-negligible in the charged states. These observations can be explained by steric crowding that supposed to hinder the local motion of the dendrimer segments. This effect can be also related to electrostatic binding of counterions ($Cl^-$ in our case). It is likely the reason for obtaining a larger diffusion coefficient at low ionic strength. A similar dependence of the diffusion coefficient on pH and ionic strength was reported by Nisato et al.[6] for G8 dendrimers.

The Stokes hydrodynamic radius of the dendrimers can be determined from the diffusion coefficient using the known relation:

$$R_H = \frac{kT}{6\pi\eta D} \tag{3}$$

An average $R_H$ value of 3.7 nm was calculated from eq 1 using the diffusion coefficients of the G6 dendrimer as a function of ionic strength (0.01−0.15 M) at pH = 9.5. This result is similar to that obtained by Jackson et al.[1] using cryo-TEM images ($R$ = 3.4 nm). The higher value of $R_H$ obtained by DLS in solution is reasonable. Maiti et al.[3,4] performed molecular dynamics (MD) simulations on the structure of G8 PAMAM (eighth-generation) dendrimers and found that a decrease in pH from 12 to 4 resulted in an increase in the radius of gyration from 3.78 to 4.31 nm. The theoretical calculations were compared to experimental measurements using SAXS and SANS. The authors found that the radius of gyration ($R$) for a generation-$N$ dendrimer varies as $R \approx N^{1/3}$. Similar work was performed by Welch and Methukumar[5] using Monte Carlo simulations. They demonstrated that the shape of the intermolecular density profile of dendrimers in solution can be tailored by varying the ionic strength or pH of the solvent. The simulation demonstrated that the density profile can transform from a dense core into a dense shell structure.

**Effective Charge.** The effective charge and its dependence on pH and ionic strength are other bulk characteristics of dendrimer solutions that are crucial for the interpretation of their adsorption and deposition characteristics. These data can be derived from electrophoretic mobility measurements. The dependence of $\mu_e$ on the pH of the PAMAM dendrimer solution was measured at three ionic strengths ($10^{-3}$, $10^{-2}$, and 0.15 M); the results are shown in Figure 1. For $I = 1 \times 10^{-3}$ M, the electrophoretic mobility decreases monotonically from $7.3 \times 10^{-8}$ m$^2$ (V·s)$^{-1}$ at pH 4.0 to 0.0 m$^2$ (V·s)$^{-1}$ at pH 9.9. The pH value when the electrophoretic mobility is zero is usually referred to as the isoelectric point (iep).

PAMAM G6 dendrimers contain primary (256) and tertiary (254) amine groups. These groups determine the protonation mechanism that is active in PAMAM dendrimers. At low pH, all of the primary and tertiary amines are protonated (pH < 4). At intermediate or neutral pH, all primary amines are protonated. At high pH, no protonation (pH > 10) is observed. These observations correspond well with the value of the isoelectric point of the dendrimer. The negative charge of the dendrimer


dx.doi.org/10.1021/jp307832p | J. Phys. Chem. C 2013, 117, 1136−1145

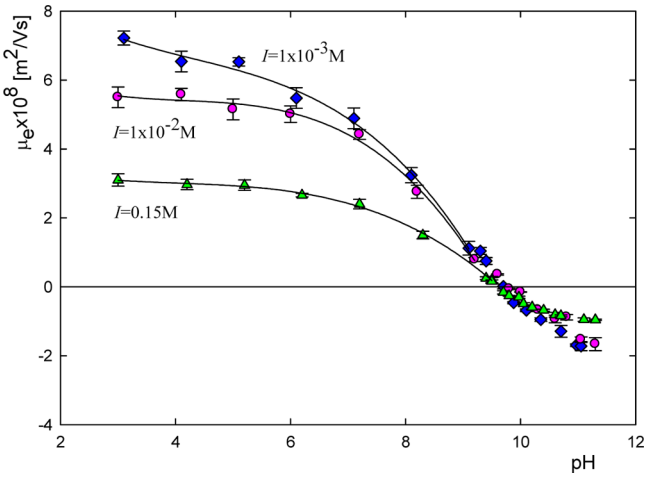


**Figure 1.** The dependence of the electrophoretic mobility $\mu_e$ of the G6 PAMAM dendrimer solution on pH at different ionic strengths. The points denote the experimental values determined for $I = 1 \times 10^{-3}$ M, $I = 1 \times 10^{-2}$ M, and $I = 0.15$ M.

observed for pH > 10 is likely caused by the specific adsorption of $OH^-$ ions. At pH = 11, the electrophoretic mobility varies from −1.7 [$\mu$m·cm·V$^{-1}$·s$^{-1}$] at $I = 1 \times 10^{-3}$ M to −0.9 [$\mu$m·cm·V$^{-1}$·s$^{-1}$] at $I = 0.15$ M, which may indicate the specific adsorption of counterions under these conditions. An analogous phenomenon was also observed for a linear weak polyelectrolyte, poly(ally amine hydrochloride) (PAH), which has primary amine groups in its main chain.[16] The general mechanism of protonation of hyperbranched polyelectrolytes was proposed by Koper et al.[19]

The effective (uncompensated) charge of dendrimer molecules, $q$, can be calculated from the electrophoretic mobility and the hydrodynamic radius using the Lorenz−Stokes equation derived in ref 20.

$$q = \frac{kT}{D}\mu_e = 6\pi\eta R_H \mu_e \quad (4)$$

where $\mu_e = \langle U\rangle/E$ and $\langle U\rangle$ is the average migration velocity of dendrimer molecules in a uniform electric field $E$. Considering that $e = 1.602 \times 10^{-19}$ C, eq 4 can be used to calculate the average number of elementary charges per molecule, $N_c$:

$$N_c = \frac{6\pi\eta R_H}{e}\mu_e \quad (5)$$

The effective degree of ionization of a molecule is given by $\alpha = N_c/N_m$, where $N_m$ is the nominal number of charges per molecule. Substituting our experimental data, that is, $\mu_e = 7.3 \times 10^{-8}$ m$^2$ (V·s)$^{-1}$ ($I = 1 \times 10^{-3}$ M) and $R_H = 3.7$ nm, one obtains $N_c = 28.3$, the average number of free charges (of positive sign) per PAMAM dendrimer molecule (Table 1). This gives an effective ionization degree of $\alpha = 0.11$ (taking into account that the nominal number of surface charges is 246). For $I = 0.15$ M, $\mu_e = 3.1 \times 10^{-8}$ m$^2$ (V·s)$^{-1}$, and $R_H = 3.7$ nm, the calculations give $N_c = 12.1$ as the maximum number of mobile charges and $\alpha = 0.046$.

The effective degree of ionization is also strongly dependent on pH and is much smaller than unity, indicating that the nominal charge of PAMAM dendrimer molecules is largely compensated. This effect can be explained by the specific adsorption of counterions, which is often referred to as the ion-condensation phenomenon.[21,22]

In carefully analyzing the literature, it become evident that qualitative explanation of the mechanism of PAMAM dendrimer protonation is not trivial. The protonation behavior of the linear chains is commonly compared to the hyperbranched polyamines like dendrimers. Such dendrimers contain primary and tertiary amine groups only, albeit in different chemical environments. As a result, the primary groups are substantially more basic than the tertiary ones. The protonation mechanism can be inferred from the site-specific titration curves. All primary amines are protonated in the basic region. Because of weak interaction, the tertiary sites protonate almost independently, and they all protonate simultaneously in more acidic condition. Such a qualitative protonation pattern was proposed for PAMAM dendrimers by Cakara et al.[23] PAMAM dendrimers of generations G0−G6 were investigated by potentiometric titration, and the data were analyzed in terms of classical macroscopic protonation equilibrium and a side binding model. The following microscopic protonation mechanism of PAMAM dendrimers was deduced from the mentioned analysis. At high pH, the primary amine groups at the outer rim of the dendrimer protonate, while the tertiary amine groups in the dendrimer core only protonate at lower pH. The last group to protonate is one of the central tertiary amine groups. They estimated the p$K_a$ value (the pH value at which 50% of the functional groups are ionized) of the G6 dendrimer to be 8.0. The respective protonations at given pH values were deduced for our dendrimers using the proposed mechanism and taking into account the relative content of primary and tertiary amine groups in the molecule.

**Table 1. Number of Uncompensated Charges $N_c$ of the G6 PAMAM Dendrimer[a]**

| $I = 1 \times 10^{-3}$ M | | | $I = 1 \times 10^{-2}$ M | | | $I = 0.15$ M | | |
|---|---|---|---|---|---|---|---|---|
| pH | $\mu_e$ | $N_c$ [e] | pH | $\mu_e$ | $N_c$ [e] | pH | $\mu_e$ | $N_c$ [e] |
| 3.1 | 7.2 | 28.3 | 3.0 | 5.5 | 21,8 | 3.0 | 3.1 | 12.2 |
| 4.1 | 6.5 | 25.6 | 4.1 | 5.6 | 21.9 | 4.2 | 3.0 | 11.7 |
| 5.1 | 6.5 | 25.6 | 5.0 | 5.1 | 20.2 | 5.2 | 2.9 | 11.6 |
| 6.1 | 5.5 | 21.5 | 6.0 | 5.0 | 19.7 | 6.2 | 2.7 | 10.4 |
| 7.1 | 4.9 | 19.2 | 7.2 | 4.4 | 17.3 | 7.2 | 2.4 | 9.4 |
| 8.1 | 3.2 | 12.7 | 8.2 | 2.8 | 10.8 | 8.3 | 1.5 | 5.9 |
| 9.1 | 1.1 | 4.4 | 9.2 | 0.8 | 3.1 | 9.5 | 0.2 | 0.8 |
| 10.1 | −0.7 | −2.7 | 10.0 | −0.1 | −0.6 | 10.0 | −0.5 | −1.9 |
| 11.0 | −1.7 | −6.6 | 11.0 | −1.5 | −6.0 | 11.1 | −0.9 | −3.7 |
| 11.0 | −1.7 | −6.7 | 11.3 | −1.5 | −5.8 | 11.3 | −0.9 | −3.7 |

[a] $T = 298$ K, $c = 2000$ ppm, $\eta = 8.9 \times 10^{-3}$ g (cm·s)$^{-1}$, $R_H = 3.7 \times 10^{-7}$ cm, $\mu_e$ in [$\mu$m·cm·V$^{-1}$·s$^{-1}$].


dx.doi.org/10.1021/jp307832p | J. Phys. Chem. C 2013, 117, 1136−1145

**Zeta Potential.** Maiti et al.[24] used MD simulations to calculate the zeta potential of PAMAM dendrimers as a function of dendrimer generation. They found that the zeta potential increases with dendrimer generation. The simulations were performed at neutral pH, assuming that all of the primary amines of the PAMAM dendrimer were protonated. For G6 PAMAM at neutral pH, the zeta potential was equal to 70 mV.

The zeta potential is related to the electrophoretic mobility via Henry's constitutive equation:

$$\zeta = \frac{3\eta}{2\varepsilon F(\kappa a)}\mu_e \tag{6}$$

where $\zeta$ is the zeta potential of the polymer, $\mu_e$ is the electrophoretic mobility, $\varepsilon$ is the dielectric constant of the solvent, $F(\kappa a)$ is a function of the dimensionless parameter $\kappa a$, $\kappa^{-1} = (\varepsilon kT/2e^2I)^{1/2}$ is the Debye length, and $a$ is the characteristic dimension of the polymer (e.g., its hydrodynamic radius). We calculated a zeta potential for $I$ = 0.15 M and a neutral pH, which are the same conditions as those used by Maiti et al.[24] Two restrictions on the use of Henry's equation are that the potential of the surface should be low (less than 25 mV), and the distortion of the electrical double layer should be minimal during particle migration in electrophoresis. In our experiments, the potential was higher than 25 mV, and we also recalculated the results using the O'Brien and White model (OBW). The zeta potentials calculated from Henry's equation and the O'Brien and White model were $\zeta_H$ = 70 mV and $\zeta_{OBW}$ = 77 mV.

The theoretical surface charge densities at the full ionization ($\alpha$ = 1) of the dendrimer can be estimated from the following formula:

$$\sigma_t = eN_c/4\pi r^2 \tag{7}$$

where $e$ is the elementary charge ($1.602 \times 10^{-19}$ C).

The effective degree of ionization of the molecule can be calculated from the electrophoretic mobility. By substituting our experimental data, that is, $N_c$ = 28.3 and $R_H$ = 3.7 nm ($I$ = $10^{-3}$ M and pH = 4.0), we obtained an experimental charge density of $\sigma_{ex}$ = 0.025 C/m$^2$ for the PAMAM molecule. Therefore, the effective surface charge density is much weaker than the apparent geometrical surface charge density, $\sigma_t$ = 0.23 C/m$^2$.

**Dynamic Viscosity.** As has been previously demonstrated for polyelectrolytes[16] and proteins,[20] some additional information regarding the shape of the particles forming suspensions and their degree of aggregation can be derived from dynamic viscosity measurements carried out at low values of the volume fraction. The dependence of the relative viscosity $\eta/\eta_s$ of a suspension (where $\eta$ is the suspension viscosity and $\eta_s$ is the solvent viscosity) on its volume fraction $\Phi$ is quantitatively related to the shape of a molecule or aggregate. The spherical shape, monodispersity, and uniform surface charge density of PAMAM dendrimers make them particularly suitable for such fundamental viscosity studies. For nonrigid and nonspherical particles, the Einstein model can be written as

$$\frac{\eta}{\eta_s} = 1 + \nu\Phi \tag{8}$$

where $\nu$ is the viscosity increment (Simha factor).

The Simha factor is related to the intrinsic viscosity $[\eta]$ and is defined as

$$[\eta]_\Phi = \lim_{\Phi\to 0}\left(\frac{\eta - \eta_s}{\eta_s\Phi}\right) = \nu \tag{9}$$

The viscosity increment, $\nu$, is referred to as a "universal shape function" and is directly related to the shape of the particle. If a macromolecule carries multiple charges, the electrostatic charge can also affect the intrinsic viscosity of the polymer solution. Three electro viscous contributions can be distinguished for polymers in solution: primary effects, the resistance of the diffusive double layer surrounding the molecule; secondary effects, the repulsions between the double layers of macromolecules; and tertiary effects, the interparticle repulsions that affect the shape of macromolecules.

The results of dynamic viscosity measurements at pH = 9.5 and ionic strength $I$ = 0.15 M are shown in Figure 2; they are

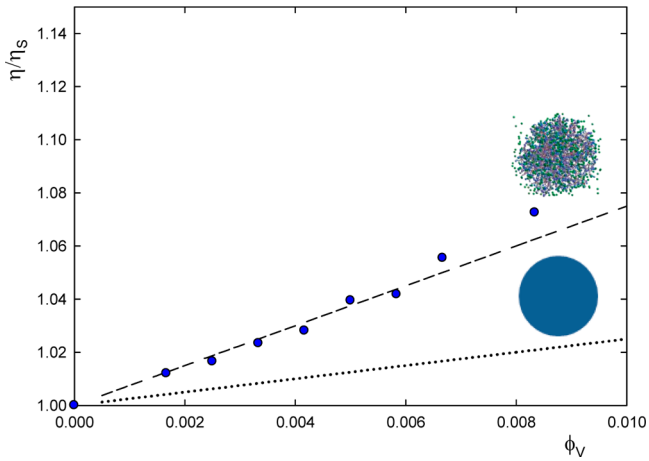


**Figure 2.** The dependence of the relative viscosity $\eta/\eta_s$ of the G6 PAMAM dendrimers on the volume fraction $\Phi_v$ at $I$ = 0.15 M and pH = 9.5. The points denote experimental data. The broken line denotes the theoretical results calculated from the Einstein formula $\eta_s/\eta = 1 + 2.5\Phi_V$, and the solid line represents the linear regression.

reported as the dependence of the relative viscosity of the PAMAM dendrimer solutions, $\eta/\eta_s$, on the volume fraction (for $\Phi$ < 0.009). The experimental results are fitted well by a linear dependence with a slope of $\nu$ = 7.5. The experimental $\nu$ value is 3 times larger than the respective coefficient in the Einstein formula (eq 8). Typically, deviations from the Einstein formula are interpreted in terms of the primary electro viscous effect according to the relationship:[25]

$$\eta/\eta_s = 1 + 2.5(1 + p)\Phi \tag{10}$$

where $p$ is the primary electro viscous function. Assuming that the ion mobilities do not vary significantly, one can express $p$ as follows:[25]

$$p = \frac{2\varepsilon\xi^2(1 + \kappa a)^2F(\kappa a)}{3\pi\eta D_i} \tag{11}$$

where $\varepsilon$ is the dielectric constant of water (relative permittivity), $D_i$ is the ion diffusion coefficient, and $F(\kappa a)$ is a function of the dimensionless $\kappa a$ parameter.

For an ionic strength of $I$ = 0.15 M and a $\kappa a$ = 4.7, the value of the function $(1 + \kappa a)^2F(\kappa a)$ equals $1 \times 10^{-3}$. With the zeta potential and size of the dendrimer, one can use eq 11 to estimate that $p = 1 \times 10^{-3}$. This value is significantly smaller than the experimental value ($p$ = 2, based on eq 11). This


dx.doi.org/10.1021/jp307832p | J. Phys. Chem. C 2013, 117, 1136−1145

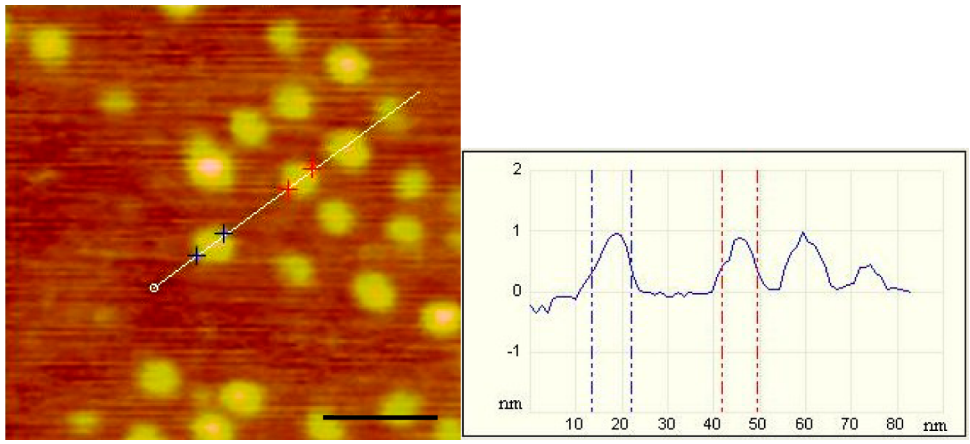


**Figure 3.** An AFM image (100 nm × 100 nm) of individual G6 PAMAM dendrimers deposited on a mica surface. The samples were prepared at pH = 6.5 and $I = 1 \times 10^{-3}$ M. The scale bar in the image represents 25 nm. The profile cross-section of the PAMAM dendrimer on the mica surface is shown at the bottom.

comparison proves that the primary electro viscous effect cannot explain the anomalous behavior of the viscosity of the dendrimer solution in the low-concentration regime. A plausible explanation for this discrepancy lies in the core/shell structure of the dendrimer particles in aqueous media, as was postulated previously.[5] According to this hypothesis, upon contact with water, a gel-like layer is formed on the surface of the dendrimer; this layer has a much lower density than the core region of the molecule. As a result, the effective hydrodynamic volume of a molecule in aqueous solution is larger than under dry conditions. This assumption was further supported by molecular dynamics simulations presented in refs 24,26, indicating that the core region is denser than the shell of the dendrimer, which is fairly sparse. The density of the molecule decreases at low ionic strength and low pH, when the double-layer thickness is large and the dendrimers are highly charged. These results may be interpreted as the swelling of the dendrimers due to interactions between the solvent molecules and the primary and tertiary amines. For PAMAM dendrimers at high pH, none of the primary and tertiary amines are protonated. At neutral pH, the primary amines are protonated, and at low pH, the primary amines and tertiary amines are protonated. The protonation of the amines, particularly the tertiary amines inside a dendrimer, attracts additional water into the dendrimer, leading to additional swelling. The interior of the G6 dendrimer is not crowded, leaving space to accommodate additional water and ions. Maiti et al.[26] estimated that at low pH the dendrimer structure is open and observed a significant penetration of solvent molecules into the interior of the dendrimer molecule. For example, at high pH, they estimated a ratio of three water molecules per tertiary amine; this number increases to six at low pH. Using SANS measurements, the average water density inside a dendrimer was estimated and found be higher than that of bulk water.[27] The number of water molecules associated with single G6 molecule was estimated to be 1728 ± 131.

Assuming that this model is valid, the apparent (effective) volume fraction $\Phi_V^*$ of the dendrimer particles can be expressed as

$$\Phi_V^* = (1 + p^*)\Phi \tag{12}$$

where $p^* = tg\alpha/2.5 - 1$ is the apparent electro viscous effect and $tg\alpha$ is the slope of $\eta/\eta_S$ versus $\Phi$.

One may suspect that a loose shell structure does not ensure the rigid wall hydrodynamic boundary conditions that are necessary for the Einstein viscosity model to be valid. Unfortunately, to the best of our knowledge, there is no quantitative model that predicts the viscosity of such composite core/shell particles. However, an analogous problem involving a uniform flow past a composite sphere has been treated both theoretically and experimentally by Masliyah et al.[28] The experimental results showed that, in accordance with theoretical predictions, a 0.8% volume fraction of threads (99.2% porosity of the layer) increased the hydrodynamic drag on the particles 2-fold. This is just 77% of the value expected for a solid particle with the same radius as the composite particle, that is, 2.6*a* (the average length of the threads was 1.6 times larger than the particle radius *a*). These experimental results strongly suggest that, for the porosity range predicted for the gel layer (i.e., 76–86%), the composite particles can be modeled as solid spheres. This is in accordance with the significantly larger hydrodynamic radius of the dendrimer spheres measured by DLS than that derived from TEM microscopy.

**Atomic Force Microscopy Imaging.** AFM topological measurements were performed on single molecules adsorbed onto bare mica at a pH of 6.5 and an ionic strength of $1 \times 10^{-3}$ M (see Figure 3). The diameter of the isolated dendrimers was measured to be approximately 5–10 nm (with some variation from different AFM tips), and their height was no greater than 1 nm. Although the actual diameters of PAMAM dendrimers adsorbed onto mica may be smaller due to convolution of the tip size, the measured height confirms that the dendrimers undergo some deformation upon adsorption. The maximum height of a single dendrimer strongly depends on the interaction between the dendrimer molecule and the substrate.[29,30] The work of Betley et al.[30] indicates that dendrimers "spread out" and flatten on the substrate surface. The researchers observed that the degree of deformation is lower for higher-generation dendrimers. Although the convolution of the AFM tip is an important imaging artifact in the diameter and volume measurements, the height information is reliable.

**Quartz Crystal Microbalance with Dissipation Monitoring (QCM-D).** The adsorption of PAMAM was followed, by using the QCM-D technique, at the two ionic strengths, $1 \times 10^{-2}$ and 0.15 M NaCl. The changes in the frequency, $\Delta f$, and


dx.doi.org/10.1021/jp307832p | J. Phys. Chem. C 2013, 117, 1136–1145

the dissipation energy, $\Delta D_{dis}$, as a function of time are illustrated in Figures 4A and B. In the preliminary experiment

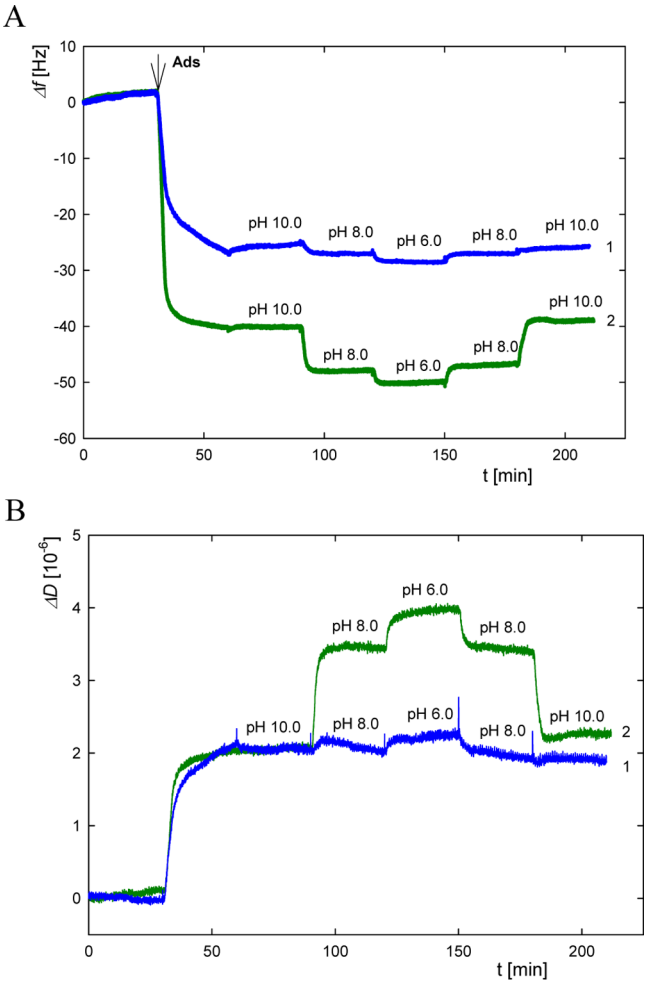


**Figure 4.** (A) The time dependence of the frequency shift ($\Delta f$) for the resonator after adsorption on a Au-coated sensor. The G6 PAMAM dendrimer concentration was $c$ = 5 ppm in a NaCl solution at the following ionic strengths: (1) $I$ = 0.15 M, (2) $I = 1 \times 10^{-2}$ M. (B) The time dependence of the dissipation shift ($\Delta D_{dis}$) for the resonator after adsorption on a Au-coated sensor. The G6 PAMAM dendrimer concentration was $c$ = 5 ppm in a NaCl solution at the following ionic strengths: (1) $I$ = 0.15 M, (2) $I = 1 \times 10^{-2}$ M.

stage, the $\Delta f$ and the $\Delta D_{dis}$ were measured for the supporting electrolyte (NaCl) solution of pH = 10. Next, a solution of PAMAM dendrimer of the concentration of $c$ = 5 ppm and pH 10, in the presence of the proper electrolyte solution, was put in flow throughout the QCM cell. It caused a decrease of the $\Delta f$ and increase of the $\Delta D_{dis}$ with time, up to reaching a plateau value. The film was then washed in flow with the supporting electrolyte (NaCl) solution of pH = 10. During this stage, only slight changes in the $\Delta f$ and the $\Delta D_{dis}$ were observed (Figure 4A,B), which clearly indicates that the dendrimer molecules were irreversibly adsorbed onto the resonant surface (Au). During the next consecutive stages, the adsorption film was contacted in flow with the supporting electrolyte (NaCl) solution of pH adjusted to 8.0, 6.0, again 8.0, and 10.0, respectively, each of the consecutive stages lasting ca. 30 min. As shown in ref 23, the degree of protonation of PAMAM molecule under these pH values amounts to ca. 0% (pH 10), 50% (pH 8), and 100% (pH 6), respectively. It does mean that, with decreasing pH, G6 PAMAM molecule varies from being uncharged at pH 10 to completely charged at pH 6. The effective charge of the dendrimer molecule in solutions is crucial for interpreting the adsorption and deposition phenomena. The charge can be estimated from the electrophoretic mobility, $\mu_e$, measurements.

The decrease in the $\Delta f$ with decreasing pH indicates the corresponding increase of mass of the film. The increased mass, under the conditions used, should be attributed to hydration of the dendrimers and trapping of water molecules into its internal voids. The amount of the bound water increases with lowering pH, which is attributed to increasing the protonation degree of the dendrimer forcing its conformation to extend more.

The proper description and control of polymer deposition requires a thorough knowledge of the dendrimer structural and transport properties, such as the molecular shape, conformational changes, degree of hydration, uncompensated charge, diffusion coefficient, and the possible aggregation phenomena.

The mass of wet dendrimer films, adsorbed onto the Au-coated sensor, increased with decreasing pH, that is, from 700 ng/cm$^2$ at pH 10 to 876 ng/cm$^2$ at pH 6.0, at the ionic strength of $I = 1 \times 10^{-2}$ M (Table 2). It indicates that the amount of water bound to the dendrimer increased by 25%, decreasing pH from 10 to 6. It is interesting that upon the pH change in the reversed sequence, the film mass was returning to the equilibrium value with respect to pH, so that it was practically the same at the start and at the end of the experiment. These results give evidence to reversibility of the hydration driven by extending the dendrimer conformation upon charging, which is discussed in terms of molecular swelling. Comparatively, the analogous results obtained at the higher ionic strength, $I$ = 0.15 M (Figure 4A), showed the same trend in the $\Delta f$ shift with pH, but increase of the wet film mass upon pH change from 10 to 6 was lower, amounting only to 15%. This indicates that incorporation of water tuned by the dendrimer charge, discussed in terms of swelling the dendrimer, decreases with the ionic strength. This effect should be attributed to screening the dendrimer surface charge by the electrolyte as a result of compressing the diffuse layer of the counterions (diminishing the Debye length). At a high electrolyte concentration, also, coadsorption of a fraction of the counterions may occur in the Helmholtz plane of the double layer formed at the dendrimer surface. The latter phenomenon is often referred to as the ion condensation phenomenon, such as that observed experimentally for polyelectrolytes.[16]

The phenomenon of swelling dendrimer films adsorbed on a $SiO_2$ surface from salt-free, aqueous solutions, was preliminarily

**Table 2. Changes in Mass and Thickness for G6 PAMAM Adsorbed on Au-Coated Sensor**

| | | $I = 1 \times 10^{-2}$ M | | | $I$ = 0.15 M | | |
|---|---|---|---|---|---|---|---|
| | | | thickness [nm] | | | thickness [nm] | |
| stage | pH | mass [ng/cm$^2$] | $\rho_{film}$ = 1.16 [g/cm$^3$] | $\rho_{film}$ = 1.11 [g/cm$^3$] | mass [ng/cm$^2$] | $\rho_{film}$ = 1.16 [g/cm$^3$] | $\rho_{film}$ = 1.13 [g/cm$^3$] |
| 1 | 10.0 | 700 | 6.0 | 6.3 | 449 | 3.9 | 4.0 |
| 2 | 8.0 | 841 | 7.2 | 7.6 | 471 | 4.0 | 4.2 |
| 3 | 6.0 | 876 | 7.5 | 7.9 | 499 | 4.3 | 4.4 |
| 4 | 8.0 | 827 | 7.1 | 7.4 | 470 | 4.0 | 4.2 |
| 5 | 10.0 | 690 | 5.9 | 6.2 | 449 | 3.9 | 4.0 |


dx.doi.org/10.1021/jp307832p | J. Phys. Chem. C 2013, 117, 1136−1145

investigated and reported for PAMAM G-10 dendrimer, using the QCM and AFM techniques.[15] Despite a number of investigations on the phenomenon, summarized in ref 15, swelling of a dendrimer adsorbed onto a solid support is far from being understood in detail, so far. As suggested in ref 15, the phenomenon is strongly influenced by the adsorbate−substrate interactions; hence, the kind of support used and its susceptibility to changing the surface charge with pH (such as that in case of $SiO_2$) may be of great influence on the results. The gold support used by us seems to be optimal with the above respect.

Mass of the adsorbed dendrimer evaluated as per unit the geometrical surface, in ng/cm$^2$, designated as Γ, according to the denotation commonly used in adsorption studies, can be evaluated from the following formula:

$$\Gamma_{ad} = \frac{M_w}{S_g A_V}\Theta \tag{13}$$

where $M_w$ is the molecular weight, $S_g$ is the cross-section area, which for the near spherical molecule is $S_g = \pi r^2 = 43$ nm$^2$ (in the case of G6 dendrimer $r = 3.7$ nm as determined by DLS measurements), $A_V$ is the Avogadro number, and Θ is the coverage. Using this definition and considering that the $M_w$ of unhydrated PAMAM G6 molecule equals 58 kDa, one can calculate that Γ = 112 ng/cm$^2$ at the maximum coverage of Θ = 0.55 (the jamming limit). Assuming that the hydration water contributes to the PAMAM molecule weight by ca. 20%, as suggested in ref 31, the mass of the saturated film, corrected for the molecule hydration, should be 135 ng/cm$^2$. The mass obtained from the QCM measurements for the adsorbed PAMAM film at pH 10.0 (i.e., when the protonation degree is negligible allowing for the relatively largest coverage) is by 6 times greater than the saturation Γ value calculated according to eq 13. This discrepancy indicates that a part of the film mass determined with the QCM technique is contributed by water bound at the interfacial areas free of the adsorbate. The other reasons for the enhanced mass of the film may be formation of multilayer areas in the dendrimer film or surface aggregation of the uncharged dendrimer (at pH 10). The latter phenomenon may cause trapping of an additional amount of water inside the aggregates.

To resolve the reason for the difference of the structure of dendrimer film formed under $I = 0.15$ M and $I = 1 \times 10^{-2}$ M ionic strength, we obtained AFM images of films, formed on the Au-coated sensor used in QCM experiments. The images are shown in Figure 5. By analysis, the topology of PAMAM dendrimer films has shown differences between the films deposited at high and low ionic strength. We can see aggregates on the Au surface. The aggregates have regular structure, and their size depends on ionic strength. This behavior nicely correlates with the effective charge of the dendrimer and its dependence on pH and ionic strength.

The QCM adsorption results were used by us to estimate thicknesses of the dendrimer films. The mass, $\Delta m$, of the wet film was calculated from the Sauerbrey relation, and it was directly converted to the film thickness, assuming the fixed density of the G-6 PAMAM dendrimers (Table 2). We propose that upon contact with water, a gel-like layer is formed on the dendrimer outer shell, which in principle is of much greater density than the dendrimer core region. Therefore, the average density of the dendrimer in water is lower than that of the crystalline state, 1.2 g/cm$^3$.[32]

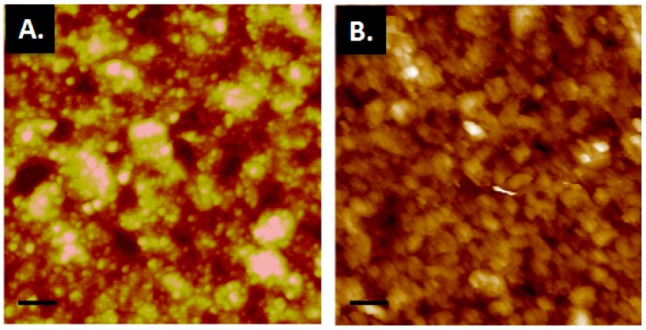


**Figure 5.** The AFM images of PAMAM dendrimer after adsorption on Au-coated sensor. The G6 PAMAM dendrimer concentration was $c$ = 5 ppm in a NaCl solution at the following ionic strengths: (A) $I = 0.15$ M and (B) $I = 1 \times 10^{-2}$ M. The scales bars in the images represent 100 nm.

The dendrimer film thickness can be calculated when one knows the density of the wet film, given by the following equation:

$$\rho_{film} = \frac{\Phi_{VD}\rho_D + \Phi_{VS}\rho_s}{\Phi_{VD} + \Phi_{VS}} \tag{14}$$

were $\rho_s$ is the density of the NaCl solution, $\rho_D$ is the density of PAMAM dendrimers, $\Phi_{VD}$ is the volume fraction of the dendrimer in solution, and $\Phi_{VS}$ is the volume fraction of water in the film. Equation 14 gives only the approximate value of $\rho_{film}$ under the assumption of ideal mixing and a homogeneous structure of the film. Equation 14 was applied by us for calculating the film densities. They have been found in the range between $\rho_{film} = 1.16$ g/cm$^3$ for pH 10.0 and $\rho_{film} = 1.11$ g/cm$^3$ for pH = 6.0, at $I = 1 \times 10^{-2}$ M. For the higher ionic strength, the film density changes from $\rho_{film} = 1.16$ g/cm$^3$ at pH 10.0 to $\rho_{film} = 1.13$ g/cm$^3$ at pH = 6.0. The determined film thickness, depending on pH, changes from 6.0 to 6.3 nm at pH 10.0, or from 7.5 to 7.9 nm at pH 6.0, at the ionic strength $I = 1 \times 10^{-2}$ M (Table 2). For the higher ionic strength, $I = 0.15$ M, the thickness changes in the range of 3.9−4.0 nm at pH 10.0, and of 4.3−4.4 nm at pH 6.0.

Reimhuit et al.[33] showed that the water mass sensed by QCM is affected not only by (1) water trapped within supramolecular assemblies or (2) the water shells surrounding the adsorbed molecules, but also by (3) water dynamically trapped between adsorbed molecules. It is difficult to separate these contributions. The content of trapped water notably increases with decreasing pH of NaCl solution contacted with the film, which suggests that the charge of the dendrimer is tuned by pH, due to protonation of tertiary amine groups. In the most intensively swollen state, at pH 6.0, the mass of the film is approximately 25% higher than that of the film at pH 10.0, although, under the latter pH, the film also contains a considerable amount of water. The increase in water content in the film is accompanied by a significant increase of the dissipation energy, shown in Figure 4B. These results support the dendrimer molecule adopting a more extended conformation with decreasing pH and lowering the ionic strength.

The dissipation energy shift, $\Delta D_{dis}$, reflects both collapse of the film and swelling of the adsorbed dendrimer molecules. When the pH decreases from pH 10.0 to pH 6.0, the $\Delta D_{dis}$ increases from 2.0 to 4.0, indicating that the dendrimer extends its conformation, that is, becomes swollen. The normalized dissipation energy, $\Delta D_{dis}/(\Delta f/n)$, reflects rigidity of the


dx.doi.org/10.1021/jp307832p | J. Phys. Chem. C 2013, 117, 1136−1145

adsorbed film. This parameter is extensively used in QCM studies to characterize the viscoelastic properties of surface films. Rigid films show a low value of $\Delta D_{dis}/(\Delta f/n)$, while flexible films show the higher one. The QCM measurement shows unquestionably that the adsorption film of the dendrimer G-6 becomes more flexible with lowering the ionic strength and pH.

## CONCLUSIONS

It has been demonstrated experimentally that the relative viscosity of dilute PAMAM dendrimer solutions, in the presence of inert electrolyte, is increasing more rapidly with the volume fraction than the Einstein formula predicts. This viscosity could not be explained in terms of the primary electro viscous effect (driven by the particle surface charge) because of the small thickness of the electric double layer, which is highly compressed at the electrolyte concentration of $c \geq 1 \times 10^{-2}$ M. The anomalous viscosity of the dendrimer solution is interpreted by us in terms of the core/shell dendrimer model.

The electrophoretic measurements performed at various pH, in the range of 6−10, and the ionic strengths, allowed us to direct determine the number of uncompensated (electrokinetic) charge on PAMAM dendrimer molecules, under the various experimental conditions. This charge is considerably smaller than the value theoretically predicted on the basis of the stoichiometric composition of 256 primary and 254 tertiary amine groups. The maximum number of free charges was found by us of 28.3 at pH = 3.0 and the ionic strength of $I = 1 \times 10^{-3}$ M NaCl, which corresponds to the degree of ionization ca. 11%. We have shown experimentally, for the first time, that the isoelectric point of PAMAM dendrimer is located at pH = 9.9.

The combined electrophoretic mobility and the QCM measurements enabled us to determine the range of swelling of dendrimer film on Au upon pH change, which corresponds to an increase in mass of 25% upon the pH change from 10.0 to 6.0 for the ionic strength $1 \times 10^{-2}$ M. Our measurements demonstrate explicitly the essential role of pH and of the ionic strength in swelling of the dendrimer molecules. This phenomenon is electrically driven by intramolecular interaction of the protonated amine groups, which result in adopting an extended molecular conformation with formation of intramolecular voids in the dendrimers, and its hydration, which also modulates the molecular charge.

Our results supply the first reliable experimental evidence that swelling of G6 generation PAMAM dendrimer is reversible. Furthermore, we showed that this process is essentially modulated by condensation of the counterions at the dendrimer surface. These findings give a valuable insight into dendrimer science and a challenge for further theoretical and experimental study, in particular, for assessing a degree of penetration of water and the counterions into dendrimer molecules, under various conditions of pH, ionic strength, and electrolyte type.

Our results have also a practical merit, because they indicate that dendrimers may be used as stimulus-responsive drug delivery carriers, which can release a trapped drug upon a conformational transition induced in the dendrimer molecule by change in pH or the ionic strength.

## AUTHOR INFORMATION

### Corresponding Author

*Tel.: +48 126395125. Fax: +48 124251923. E-mail: ncjachim@cyf-kr.edu.pl.

### Notes

The authors declare no competing financial interest.

## ACKNOWLEDGMENTS

This work was supported by Grant MNiSzW N204 028536.

This publication is dedicated to Professor Andrzej Pomianowski on the occasion of his 90th birthday.

## REFERENCES

(1) Jackson, C. L.; Chanzy, H. D.; Booy, F. P.; Drake, B. J.; Tomalia, D. A.; Bauer, B. J.; Amis, E. J. *Macromolecules* **1998**, *31*, 6259−6265.
(2) Caminade, A. M.; Laurent, R.; Majoral, J. P. *Adv. Drug Delivery Rev.* **2005**, *57*, 2130−2146.
(3) Maiti, P. K.; Goddard, W. A., III. *J. Phys. Chem. B* **2006**, *110*, 25628−25632.
(4) Maiti, P. K.; Cagin, T.; Wang, G.; Goddard, W. A., III. *Macromolecules* **2004**, *37*, 6236−6254.
(5) Welch, P.; Muthukumar, M. *Macromolecules* **1998**, *31*, 5892−5897.
(6) Nisato, G.; Ivkov, R.; Amis, E. J. *Macromolecules* **2000**, *33*, 4172−4176.
(7) Prosa, T. J.; Bauer, B. J.; Amis, E. J.; Tomalia, D. A.; Scherrenberg, R. *J. Polym. Sci., Part B: Polym. Phys.* **1997**, *35*, 2913−2924.
(8) Pericet-Camara, R.; Papastavrou, G.; Borkovec, M. *Macromolecules* **2009**, *42*, 1749−1758.
(9) Liu, Y.; Chen, Ch.-Y.; Chen, H.-L.; Hong, K.; Shew, Ch.-Y.; Li, X.; Liu, L.; Meinichenko, Y. B.; Smith, G. S.; Herwig, K. W.; Porcar, L.; Chen, W.-R. *J. Phys. Chem. Lett.* **2010**, *1*, 2020−2024.
(10) Kihara, F.; Arima, H.; Tsutsumi, T.; Hirayama, F.; Uekama, K. *Bioconjugate Chem.* **2002**, *13*, 1211−1219.
(11) Hiraiwa, D.; Yoshimura, T.; Esumi, K. *J. Colloid Interface Sci.* **2006**, *298*, 982−986.
(12) Tomita, S.; Sato, K.; Anzai, J. *J. Colloid Interface Sci.* **2008**, *326*, 35−40.
(13) Katzur, V.; Eichler, M.; Deigele, E.; Stage, Ch.; Karageorgiev, P.; Geis-Gerstorfer, J.; Schmalz, G.; Ruhl, S.; Muller, R. *J. Colloid Interface Sci.* **2012**, *366*, 179−190.
(14) Chen, S.; Yu, Q.; Li, L.; Boozer, Ch. L.; Homola, J.; Yee, S. S.; Jiang, S. *J. Am. Chem. Soc.* **2002**, *124*, 3395−3401.
(15) Muresan, L.; Maroni, P.; Porus, M.; Longtin, R.; Papastavrous, G.; Borkovec, M. *Macromolecules* **2011**, *44*, 5069−70.
(16) Jachimska, B.; Jasiński, T.; Warszyński, P.; Adamczyk, Z. *Colloids Surf., A* **2010**, *355*, 7−15.
(17) Roach, P.; Farrer, D.; Perry, C. C. *J. Am. Chem. Soc.* **2005**, *127*, 8168−8173.
(18) Elzbieciak, M.; Zapotoczny, S.; Nowak, P.; Krastev, R.; Nowakowska, M.; Warszyński, P. *Langmuir* **2009**, *25*, 3255−3259.
(19) Koper, G. J. M.; Borkovec, M. *Polymer* **2010**, *51*, 5649−5662.
(20) Jachimska, B.; Wasilewska, M.; Adamczyk, Z. *Langmuir* **2008**, *24*, 6866−6872.
(21) Manning, G. S. *J. Chem. Phys.* **1969**, *51*, 924−933.
(22) Huang, Q. R.; Dubin, P. L.; Moorefield, C. N.; Newkome, G. R. *J. Phys. Chem. B* **2000**, *104*, 898−9049.
(23) Cakara, D.; Kleimann, J.; Borkovec, M. *Macromolecules* **2003**, *36*, 4201−4207.
(24) Maiti, P. K.; Messina, R. *Macromolecules* **2008**, *41*, 5002−5006.
(25) Laven, J.; Stein, H. N. *J. Colloid Interface Sci.* **2001**, *238*, 8−15.
(26) Maiti, P. K.; Cagin, T.; Wang, G.; Goddard, W. A., III. *Macromolecules* **2005**, *38*, 979−991.
(27) Li, T.; Hong, K.; Porcar, L.; Verduzco, R.; Butler, P. D.; Smith, G. S.; Liu, Y.; Chem, W. R. *Macromolecules* **2008**, *41*, 8916−8920.
(28) Masliyah, J. H.; Neale, G.; Małysa, K.; van der Ven, T. G. M. *Chem. Eng. Sci.* **1987**, *42*, 245−253.
(29) Li, J.; Piehler, L. T.; Qin, D.; Baker, J. R.; Tomalia, D. A.; Meier, D. J. *Langmuir* **2000**, *16*, 5613−5616.
(30) Betley, T. A.; Banaszak Holl, M. M.; Orr, B. G.; Swanson, D. R.; Tomalia, D. A.; Baker, J. R. *Langmuir* **2001**, *17*, 2768−2773.

(31) Lin, S. T.; Maiti, P. K.; Goddard, W. A., III. *J. Phys. Chem. B* **2005**, *109*, 8663−8672.
(32) Betley, T. A.; Hessler, J. A.; Mecke, A.; Banaszak Holl, M. M.; Orr, B. G.; Uppuluri, S.; Tomalia, D. A.; Baker, J. R. *Langmuir* **2002**, *18*, 3127−3133.
(33) Reimhuit, E.; Larsson, Ch.; Kasemo, B.; Hook, F. *Anal. Chem.* **2004**, *76*, 7211−722.